IAV2004 - PREPRINTS
5th IFAC/EURON Symposium on Intelligent Autonomous Vehicles
Instituto Superior Técnico, Lisboa, Portugal
July 5-7, 2004

ACCURATE AUTOMATIC GUIDANCE OF AN URBAN ELECTRIC VEHICLE RELYING ON A KINEMATIC GPS SENSOR

Benoit Thuilot *, Jonathan Bom *, François Marmoiton * and Philippe Martinet *

* *LASMEA, 24 av. des Landais, 63177 Aubière Cedex, FRANCE*
Firstname.Lastname@lasmea.univ-bpclermont.fr

Abstract: Automatic guidance of urban electric vehicles is addressed in this paper. It is shown that nonlinear control design (namely chained form conversion) and the use of a RTK GPS sensor allow to achieve curved path following with a very high accuracy. Extensive experiments, carried out with a Cycab vehicle, are discussed.

Keywords: urban automated vehicles, nonlinear control law, GPS, experiments.

1. INTRODUCTION

Saturation of vehicles traffic in large cities is a major concern. Improvements can be gained from the development of alternative public transportation systems. In order to meet public expectations, such systems should be very flexible, in order to be a suitable answer to many different individual needs, and as nuisance free as possible (with respect to pollution, noise, urban scenery, ...). Individual electric vehicles, available in a car-sharing concept, meet clearly both requirements. They appear to be very suitable in specific areas where the public demand is properly structured, as in airport terminals, attraction resorts, or inner-cities pedestrian zones, ... Full-scale experiments have already been conducted, e.g. Praxitèle in France, IntelliShare in the USA, Crayon in Japan, ...

In order to spread such a transportation system, automatic guidance of those vehicles has to be addressed: passengers could then move from any point to any other point at their convenience in an automatic way, and vehicles could be brought back autonomously to stations for refilling and reuse. Some solutions requiring an equipped environment have been proposed: an automatic bus detecting magnets laid on the ground is described in (de Graaf, 2002), vision-based control detecting beacons or road-lanes is presented *resp.* in (Sika and Pauwelussen, 2002) and (Sotelo, 2003),...

Kinematic GPS sensor (also named RTK GPS) proposes an attractive alternative to these sensing systems since, on one hand, it can provide realtime vehicle localization with a centimeter accuracy, and on the other hand, it offers a full flexibility since the path to be followed can be modified at will (since no beacon or marker has to be moved). Preliminary results of bus guidance relying on RTK GPS sensor have recently been presented in (Ward *et al.*, 2003).

In this paper, guidance of an electric vehicle relying on a unique RTK GPS sensor is demonstrated. Control law design relies on nonlinear control theory (namely chained forms). Therefore, nonlinear features of the control problem, proceeding e.g. from the curvature of the reference path, or from large initial errors, can be handled explicitly in a very precise way. A vehicle sound behaviour can then be guaranteed in any situation, and guidance accuracy is close to excellent RTK GPS accuracy.

The paper is organized as follows: the experimental setup is described in Section 2. Vehicle modelling, control law design and state reconstruction are presented in Sections 3, 4 and 5. Extensive experimental results are then reported in Section 6.

2. EXPERIMENTAL VEHICLE

Fig. 1. Cycab experimental vehicle

Our experimental vehicle is depicted on Figure 1. It is an urban electric vehicle, named Cycab, manufactured by Robosoft company. Two passengers can travel aboard at 18 $km.h^{-1}$. The 4 DC motors are powered by lead-acid batteries, providing a 2 hours autonomy. Guidance algorithms are implemented in C^{++} language on a Pentium based computer using RTAI-Linux OS. Currently, Cycab mainly serves as development products in research institutes interested in intelligent vehicles in France (INRIA) or in Singapore (NTU). However, it has already met public during full-scale experiments as Saint-Germain en Laye (France, INRIA Imara) or Nancy (France, INRIA Loria).

The RTK GPS receiver is a Thales Navigation dual frequency "Aquarius 5002" unit, providing position (and velocity) measurements with a 2 cm accuracy, at a 10 Hz sampling frequency. The GPS antenna is located on the top of the cabin. The differential corrections are received via the UHF antenna placed ahead of the Cycab.

3. VEHICLE MODELLING

Cycab vehicles are devoted to urban transportation, i.e. they move on asphalt even grounds at rather slow speeds (18 $km.h^{-1}$ in our application). Therefore, it appears quite natural to rely on a *kinematic model*, and to assume *pure rolling and non slipping* at wheel-ground contact. In such cases, vehicle modelling is commonly achieved (see for instance (The Zodiac, 1996)) relying on Ackermann's model, also named bicycle model: the two front wheels and the two rear wheels of the vehicle are considered equivalent as unique virtual wheels located at mid-distance between actual front wheels and actual rear wheels, see Figure 2.

Since the control objective is that the vehicle follows a reference path $\mathcal{R}$, we propose here to describe its configuration with respect to that path, rather than with respect to an absolute frame

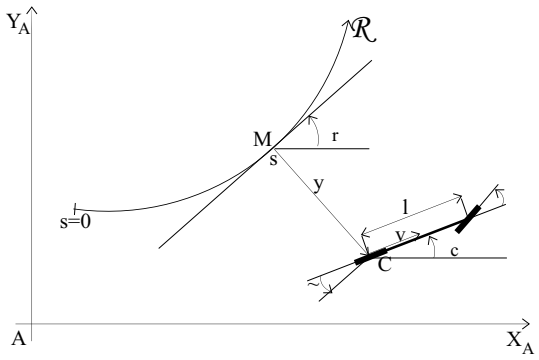

Fig. 2. Kinematic model of Cycab vehicle

$[A, X_A, Y_A)$. To meet this objective, the following notations are introduced (see also Figure 2):

- $\mathcal{R}$ is the path to be followed,
- C is the center of Cycab rear axle,
- M is the point on $\mathcal{R}$ which is the closest to C. M is assumed to be unique, which is realistic when the vehicle remains quite close from $\mathcal{R}$.
- s is the curvilinear coordinate of point M along $\mathcal{R}$, and $c(s)$ denotes the curvature of $\mathcal{R}$ at that point.
- y and $\tilde{\varphi} = \varphi_c - \varphi_r(s)$ are respectively lateral and angular deviation of the vehicle with respect to reference path $\mathcal{R}$ (see Figure 2).
- δ is the virtual front wheel steering angle.
- v is the vehicle linear velocity, considered here as a parameter, whose value may be time-varying during the vehicle evolution.
- l is the vehicle wheelbase.

Vehicle configuration can be described without ambiguity by the state vector $(s,\ y,\ \tilde{\varphi})$: the two first variables provide point C location, and the last one describes the vehicle heading. Since v is considered as a parameter, the only control variable available to achieve path following is δ.

Vehicle kinematic model can then be derived by writing that velocity vectors at point C and at the center of the front wheel are directed along wheel planes (due to non slipping assumptions), and that the vehicle motion is, at each instant, a rotation around an instantaneous rotation center (located at infinity in the translation case). Such calculations lead to (see e.g. (The Zodiac, 1996)):

$$\begin{cases} \dot{s} = \dfrac{v\cos\tilde{\varphi}}{1 - c(s)\,y} \\ \dot{y} = v\sin\tilde{\varphi} \\ \dot{\tilde{\varphi}} = v\left(\dfrac{\tan\delta}{l} - \dfrac{c(s)\cos\tilde{\varphi}}{1 - c(s)\,y}\right) \end{cases} \tag{1}$$

Model (1) is clearly singular when $y = \frac{1}{c(s)}$, i.e. when point C is superposed with the path $\mathcal{R}$ curvature center at abscissa s. However, this configuration is never encountered in practical situations: on one hand, the path curvature is small, and on the other hand, the Cycab is expected to remain close to $\mathcal{R}$.

4. CONTROL LAW DESIGN

This paper addresses path following. In view of Section 3, the control objective is to ensure the convergence of y and $\tilde{\varphi}$ to 0, independently from variable s evolution (which mainly depends on the value of parameter v).

Vehicle model (1) is clearly nonlinear. However, it has been established in (Samson, 1995) that mobile robot models can generally be converted *in an exact way* into almost linear models, named chained forms. This property offers two very attractive features: on one hand, path following control law can be designed and tuned according to celebrated Linear System Theory, while controlling nevertheless the actual nonlinear vehicle model. Control law convergence and performances are then guaranteed whatever the vehicle initial configuration is, contrarily to what was obtained with tangent linearization techniques (since in that latter case, the linear control law was designed only on an *approximation* of the actual nonlinear system). On the other hand, chained form enables to specify, in a very natural way, control law performances in term of the distance covered by the vehicle, rather than in term of time. Vehicle spatial trajectories can then easily be controlled, whatever the vehicle velocity is.

Conversion of vehicle model (1) into chained form can be achieved thanks to the following state and control transformations:

state transformation:

$$(a_1, a_2, a_3) = \Theta((s, y, \tilde{\varphi})) \triangleq (s, y, (1 - c(s)\, y) \tan \tilde{\varphi}) \quad (2)$$

control transformation $(m_1, m_2) = \Upsilon(v, \delta)$ *with:*

$$m_1 \triangleq v \frac{\cos \tilde{\varphi}}{1 - c(s)\, y} \quad (3)$$

$$m_2 \triangleq \frac{d}{dt}((1 - c(s)\, y) \tan \tilde{\varphi}) \quad (4)$$

$$= -c(s)\, v \sin \tilde{\varphi} \tan \tilde{\varphi} - \frac{d\, c(s)}{d\, s} \frac{v \cos \tilde{\varphi}}{1 - c(s)\, y} \tan \tilde{\varphi}\, y + v \frac{(1 - c(s)\, y)}{\cos^2 \tilde{\varphi}} \left(\frac{\tan \delta}{l} - c(s) \frac{\cos \tilde{\varphi}}{1 - c(s)\, y} \right)$$

The proof is straightforward: reporting (2), (3) and (4) into (1) establishes that nonlinear model (1) can be rewritten, without any approximation, as the standard chained form:

$$\begin{cases} \dot{a}_1 = m_1 \\ \dot{a}_2 = a_3\, m_1 \\ \dot{a}_3 = m_2 \end{cases} \quad (5)$$

The linear structure of chained form (5) can be revealed by replacing time derivation by a derivation with respect to the state variable a_1. Let us introduce the notations:

$$\frac{d}{d\, a_1} a_i = a_i' \qquad \text{and} \qquad m_3 = \frac{m_2}{m_1} \quad (6)$$

Reporting (6) in (5) leads to the following linear system (since the first equation has vanished):

$$\begin{cases} a_2' = a_3 \\ a_3' = m_3 \end{cases} \quad (7)$$

Chained transformations (2), (3) and (4) are invertible as long as $y \neq \frac{1}{c(s)}$ (model singularity), $v \neq 0$, and $\tilde{\varphi} \neq \frac{\pi}{2}\ [\pi]$. From a practical point of view, once properly initialized, the guided vehicle respects these conditions.

Path following can now be easily addressed: in view of (2), the desired convergence of y and $\tilde{\varphi}$ to 0 is equivalent to those of a_2 and a_3. Convergence of these two latter variables can easily be achieved by designing auxiliary control input m_3 as:

$$m_3 = -K_d\, a_3 - K_p\, a_2 \qquad (K_p, K_d) \in \mathcal{R}^{+2} \quad (8)$$

since, reporting (8) in (7), provide with:

$$a_2'' + K_d\, a_2' + K_p\, a_2 = 0 \quad (9)$$

Moreover, since derivations in error equation (9) are not time derivations, but derivations with respect to the distance $a_1 = s$ covered by the vehicle along reference path $\mathcal{R}$, the gains $(K_d,\ K_p)$ can be adjusted to specify a settling distance (instead of a settling time). Consequently, for a given initial error, the vehicle trajectory is identical, whatever the value of v is, and even if v is time-varying. Path following performances are therefore velocity independent, as desired.

The expression of the actual control law δ can finally be obtained by inverting chained transformations: reporting (8) in (6), (4), (3) and (2) provides with:

$$\delta(y, \tilde{\varphi}) = \arctan \Big(l \Big[\frac{\cos^3 \tilde{\varphi}}{(1 - c(s)\, y)^2} \Big(\frac{d\, c(s)}{d\, s}\, y \tan \tilde{\varphi} - K_d\, (1 - c(s)\, y) \tan \tilde{\varphi} - K_p\, y + c(s)\, (1 - c(s)\, y) \tan^2 \tilde{\varphi} \Big) + \frac{c(s) \cos \tilde{\varphi}}{1 - c(s)\, y} \Big] \Big) \quad (10)$$

5. STATE RECONSTRUCTION

Control law (10) requires realtime measurement of y and $\tilde{\varphi}$. As mentioned in Section 2, the only exteroceptive sensor embarked on the Cycab is a RTK GPS. Since the antenna is located on the top of the cabin, straight up the point C, absolute position and velocity of that point are then available in a direct way.

From the absolute position of point C and the knowledge of the reference path $\mathcal{R}$, the location of point M, and therefore the value of y, can be straightforwardly inferred, see Figure 2.

Obtaining state variable $\tilde{\varphi}$ proposes more difficulties. Since non-slipping has been assumed, the Cycab heading with respect to the absolute frame $[A,\ X_A,\ Y_A)$, hereafter denoted φ_c, can be inferred

from the point C absolute velocity (denoted (V_{C,X_A}, V_{C,Y_A})) also provided by the GPS:

$$\varphi_c = \begin{cases} \arctan \dfrac{V_{C,Y_A}}{V_{C,X_A}} & \text{if } V_{C,X_A} \neq 0, \\ \text{sign}(V_{C,Y_A}) \dfrac{\pi}{2} & \text{if } V_{C,X_A} = 0 \end{cases} \quad (11)$$

The value of $\tilde{\varphi}$ can then be deduced from:

$$\tilde{\varphi} = \varphi_c - \varphi_r(s) \quad (12)$$

where $\varphi_r(s)$ denotes the direction of the tangent to reference path $\mathcal{R}$ at the curvilinear coordinate s (inferred from point C absolute position provided by the GPS).

Unfortunately, experiments have shown that direct measurement (12) provides prohibitive noisy values of $\tilde{\varphi}$. A low pass filter could be considered. However, since the vehicle model is available, a suitable alternative consists in using it through a Kalman state reconstructor. Discretizing the third equation of Cycab model (1) leads to:

$$\varphi_{c,[k+1]} = \varphi_{c,[k]} + \frac{v\,T_s}{l} \tan \delta_k \quad (13)$$

where T_s is the sampling period. Celebrated Kalman state reconstructor equations provide then with (see for instance (Gelb, 1974)):

$$\begin{cases} \bar{\varphi}_{c,[k]} = \hat{\varphi}_{c,[k-1]} + \dfrac{v\,T_s}{l} \tan \delta(y_{[k-1]}, \hat{\varphi}_{c,[k-1]}) \\ \hat{\varphi}_{c,[k]} = \bar{\varphi}_{c,[k]} + L\,(\varphi^m_{c,[k]} - \bar{\varphi}_{c,[k]}) \end{cases} \quad (14)$$

L is the scalar Kalman gain, to be chosen with respect to the sensor noise features. $\varphi^m_{c,[k]}$ denotes the direct measurement of φ_c, according to (11), at time $t_k = k\,T_s$. $\hat{\varphi}_{c,[k]}$ is its filtered value at the same time, to be used in control law (10).

6. EXPERIMENTATIONS

Experimentations have been carried out with the Cycab vehicle, presented in Section 2 on the campus of Clermont-Ferrand University, France.

6.1 Straight line following

To highlight performances of control law (10), straight line following has first been achieved.

Results depicted on Figure 3 present straight line following at related velocities, from 3.6 $km.h^{-1}$ to 12.4 $km.h^{-1}$. The Cycab vehicle is initially 2 m away from reference line $\mathcal{R}$ with a correct initial heading (i.e. $y_0 \approx -2$ m and $\tilde{\varphi}_0 \approx 0°$). Control gains (K_d, K_p) have been tuned [1] to impose that lateral deviation converges to 0 (to within 5%) in 15 m. Kalman gain L has been set to 0.08 in view of sensor noise features.

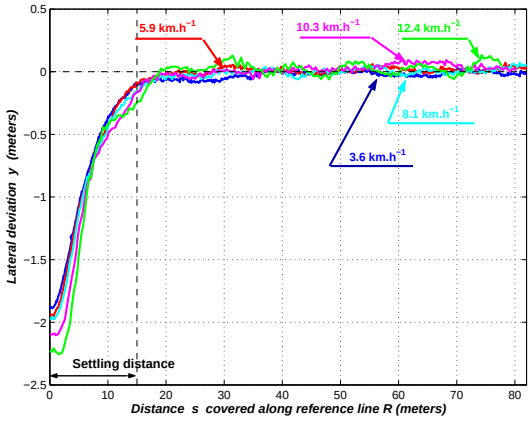

Fig. 3. Straight line following: evolution of lateral deviation y at related velocity

It can be observed that the five trajectories almost perfectly overlap: as expected from Section 4, the Cycab trajectory is independent from its velocity.

The specified settling distance can also be checked: at low velocities ($v = 3.6$ $km.h^{-1}$ or $v = 5.9$ $km.h^{-1}$), Cycab lateral deviation at $s = 15$ m is exactly $0.05 \times y_0 = -0.1$ m, as expected. Slight differences can be noted at highest velocities, due to the delays introduced by the actuators and by the Kalman state reconstructor (at $v = 12.4$ $km.h^{-1}$, the Cycab covers 15 m within 4.5 sec!).

To investigate straight line guidance accuracy, the lateral deviation mean value $\bar{y}$ (in m) and its standard deviation from the mean $std(y)$ when the Cycab has converged to the reference line $\mathcal{R}$ (precisely, when $s > 36$ m), have been reported in Table 1. It can be stressed that the order of magnitude of $\bar{y}$ and $std(y)$ is the sensor accuracy, i.e. 2 cm. Performances are slightly altered at highest velocities due to the delays over-mentioned.

v	3.6	5.9	8.1	10.3	12.4
$\bar{y}$	-0.011	0.015	0.007	0.035	0.023
$std(y)$	0.015	0.021	0.026	0.027	0.044

Table 1. Straight line guidance accuracy at related velocities

The relevancy of angular deviation reconstruction presented in Section 5 is illustrated on Figure 4. Evolutions of $\tilde{\varphi}$ derived either from direct velocities measurements (i.e. according to (11)), or through Kalman state reconstructor (14) have been recorded during straight line following at 3.6 $km.h^{-1}$. Direct measurements are clearly too noisy to be used to feed control law (10). Kalman state reconstructor (14) provides with more satisfactory values of $\tilde{\varphi}$ without introducing prohibitive delay.

[1] More precisely, (K_d, K_p) have been set to (0.6, 0.09) in order that error equation (9) presents a double pole located at value 0.3. Linear control tools ensure then that the 5% settling distance is 15 m

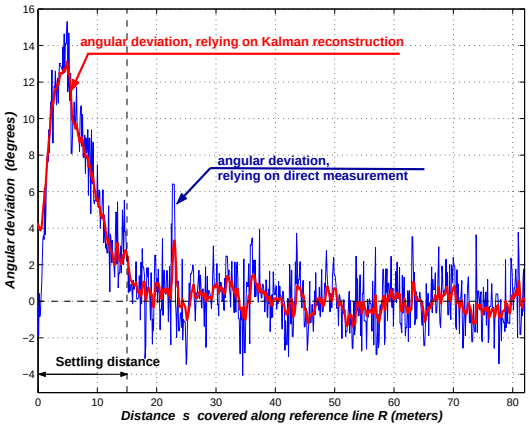

Fig. 4. Evolution of $\tilde{\varphi}$ derived via (11) or via (14) during straight line following at 3.6 $km.h^{-1}$

From a quantitative point of view, standard deviation from the mean of $\tilde{\varphi}$ when the Cycab has converged to the reference line $\mathcal{R}$ (precisely, when $s > 36\ m$) have been computed with $\tilde{\varphi}$ values provided either from direct measurement (11) or from Kalman state reconstructor (14). Results displayed in Table 2 for related vehicle velocities establish Kalman state reconstructor relevancy.

v	3.6	5.9	8.1	10.3	12.4
$std(\tilde{\varphi})$ with (11)	1.35	1.05	1.09	0.9	1.3
$std(\tilde{\varphi})$ with (14)	0.55	0.40	0.43	0.40	0.50

Table 2. $Std(\tilde{\varphi})$ (in degrees) at related velocities, when using (11) or (14).

It can however be noticed that accuracy of $\tilde{\varphi}$ estimation decreases with the vehicle velocity v. It was expected: for the lowest velocity, point C displacement during a sampling period is 10 cm. Since GPS accuracy is 2 cm, determination of vehicle heading can no longer be precise. On the contrary, the large $std(\tilde{\varphi})$ value obtained at high velocity ensues from slight oscillations in Cycab trajectory due to the over-mentioned delays.

Figure 3 has shown that Cycab trajectories are independent from its velocity, when this velocity is constant. However, since the evolution of lateral deviation (9) is specified with respect to the distance s covered along reference path $\mathcal{R}$, it is expected that Cycab trajectory remains unchanged, even if v is varying. Figure 5 displays the experimental verification: Cycab trajectories almost perfectly overlap, when $v = 3.6\ km.h^{-1}$, $v = 5.9\ km.h^{-1}$, and when v is increased from 3.6 $km.h^{-1}$ to 5.9 $km.h^{-1}$ during Cycab convergence to reference path $\mathcal{R}$.

Finally, Figure 6 highlights one of the major advantages of the exact linearization approach used to design control law (10): since no approximation (such as $\sin\tilde{\varphi} \approx \tilde{\varphi}$ e.g.) has been introduced when designing control law (10), the evolution of lateral deviation is described *in an exact way* by

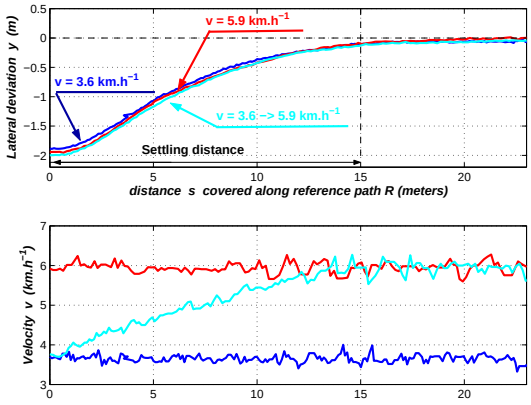

Fig. 5. Straight line following at constant and at varying velocities

equation (9), even if y and $\tilde{\varphi}$ are large. Therefore, it is expected that Cycab trajectories remain stable, and moreover consistent, even if vehicle initial configuration presents large deviation (y_0 and/or $\tilde{\varphi}_0$) with respect to the reference line $\mathcal{R}$. These performances are demonstrated on Figure 6, which displays Cycab trajectories and lateral deviation evolution from the following sets of initial conditions (Cycab velocity is 5.9 $km.h^{-1}$):

blue curve : $(y_0, \tilde{\varphi}_0) = (-2\,m,\ 0°)$ (as previously)
magenta curve : $(y_0, \tilde{\varphi}_0) = (-4\,m,\ 45°)$
cyan curve : $(y_0, \tilde{\varphi}_0) = (-2\,m,\ -45°)$
red curve : $(y_0, \tilde{\varphi}_0) = (-12\,m,\ 90°)$

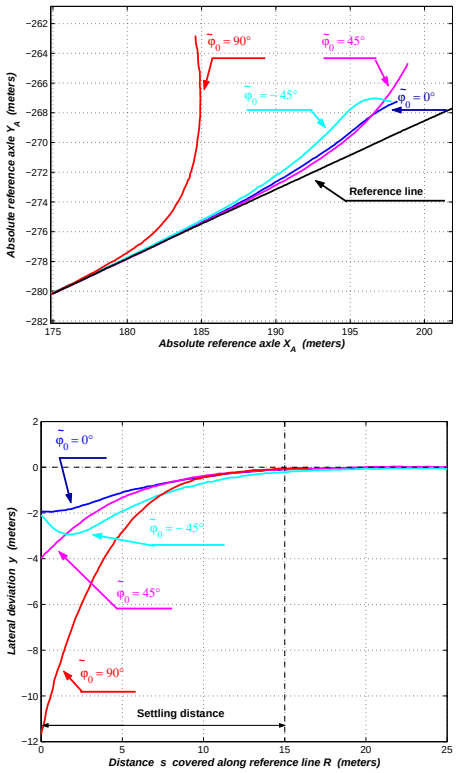

Fig. 6. Cycab trajectories and lateral deviation evolution when initial configurations are large

It can be observed that the Cycab always converges to the reference line $\mathcal{R}$ in a natural fashion,

and with the specified settling distance (i.e. 15 m). It must be emphasized that this settling distance is expressed with respect to the distance s covered along reference path $\mathcal{R}$, and not with respect to the distance covered by the Cycab: the two distances are different, especially in the red experiment. Finally, a precise look at the cyan experiment shows that the settling distance is slightly superior to 15 m: it is due to the saturation of steering actuator at the beginning of the motion.

6.2 Curved path following

Cycab nonlinear model (1) describes vehicle evolution with respect to any arbitrary curved path. Since control law design relies on exact linearization approach, no approximation on the curvature term $c(s)$ has been introduced: therefore it is expected that curved path following performances are identical to straight line following ones.

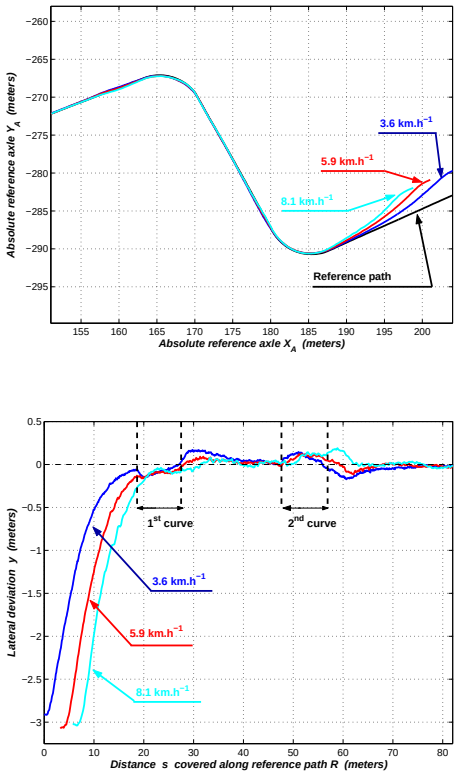

Fig. 7. Cycab trajectories and lateral deviation evolution during curved path following

Experiments reported on Figure 7 consist in automatic guidance at related velocities (from 3.6 $km.h^{-1}$ to 8.1 $km.h^{-1}$) along streets intersecting perpendicularly. On the top figure, curved path following capabilities appear very satisfactory. Evolutions of lateral deviation shown on the bottom figure enable accurate analysis: firstly, Cycab initial locations are not the same, and in one experiment, convergence of y to 0, started during straight line part of the path, is ended during the 1^{st} curve. As expected, it can be checked that decrease of y is not at all altered by entering the curve. Secondly, in all experiments, the Cycab follows the reference line when entering the 2^{nd} curve. Transient lateral errors are then observed at the beginning and at the end of the curve. They are due, on one hand, to the discontinuity of curvature term $c(s)$ at those points, and on the other hand, to the delay introduced by the steering actuator. One way to reduce such behaviour could be to anticipate the beginning and the end of the curved parts, e.g. via predictive control (this seems accessible since all reference path is known).

7. CONCLUSION

In this paper, automatic guidance of an urban electric vehicle, relying on a unique RTK GPS sensor has been addressed. A nonlinear control law has been designed, relying on chained forms. It is fed with direct position measurements and heading variable is provided by a Kalman state reconstructor. Accuracy of this guidance system has been extensively discussed from straight line and curved path following experimental results.

Improvements can still be gained by introducing anticipatory terms inside guidance law in order to reduce transient error at the beginning or the end of curves. We are also currently working on platooning: since RTK GPS sensors are expensive devices, a solution to bring vehicles back to stations could be a GPS guided Cycab pulling other vehicles in a train-like fashion by means of vision. The difficulty is to ensure stability of large platoons.

ACKNOWLEDGEMENTS

The results presented in this paper have benefited from joint work with Cemagref (Aubière, France). It is partially supported by Région Auvergne (TIMS program).

REFERENCES

de Graaf, A.J. (2002). Architecture of a generic vehicle controller. In: *Intern. Symp. on Intelligent Vehicles (IV)*. Versailles, France.

Gelb, A. (1974). *Applied optimal estimation*. MIT Press.

Samson, C. (1995). Control of chained systems. application to path following and time-varying point-stabilization of mobile robots. *IEEE Trans. on Automatic Control* **40**(1), 64–77.

Sika, J. and J. Pauwelussen (2002). Entering an automated platoon. In: *Intern. Symp. on Advanced Vehicle Control (AVEC)*. Japan.

Sotelo, M.A. (2003). Nonlinear lateral control of vision driven autonomous vehicles. In: *11^{th} Intern. Conf. on Advanced Robotics (ICAR)*. Coimbra, Portugal. pp. 1544–1549.

The Zodiac (1996). *Theory of robot control*. C. Canudas de Wit, B. Siciliano and G. Bastin Eds. Springer-Verlag, Berlin.

Ward, N., C Shankwitz, A. Gorjestani, M. Donath, E. Boer and D. DeWaard (2003). Bus rapid transit lane assist technology systems. Technical report. ITS Institute. University of Minnesota, USA.